Analysis of a Rotating Machine Flexibly Supported by Vibration Isolating Materials

Hiroyuki Fujiwara(✉), Keiji Watanabe, and Shigeharu Hayashi

National Defense Academy, 1-10-20 Hashirimizu, Yokosuka,
Kanagawa 239-8686, Japan
hiroyuki@nda.ac.jp

Abstract. When diagnosing the vibration of a rotating machine flexibly supported by vibration isolating material, the natural frequency of the rigid body mode of the machine must be considered, in addition to the natural frequency of the rotating shaft. There are two kinds of vibration isolating materials; one has a fixed spring constant, giving it the characteristic of a linear spring, and the other has nonlinear characteristics in which the spring constant varies with the mass of the machine. When the machine is supported by a linear spring, since the natural frequency varies depending on the mass of the machine, avoiding resonance requires optimal setting of the rotation speed or selection of an appropriate vibration isolating material for the equipment to be used. Meanwhile, some nonlinear springs have constant natural frequencies even if the mass of the machine changes. As the mass of the machine increases, the spring constant also increases. Selection of such a vibration isolating material is easy, because the resonance frequency is known in advance. In this study, we analyze the vibration of a rotating machine flexibly supported by vibration isolating material. Vibration analysis was carried out on a simple model of a rotating machine supported by a linear spring or a nonlinear spring. Subsequently, the experimental equipment was manufactured and numerical calculations were performed by using the derived numerical model.

Keywords: Condition monitoring · Rotating machine · Flexibly support
Vibration isolating material

1 Introduction

For monitoring vibration as a method of monitoring the condition of rotation machinery (electric motor, pump), ISO 10816 [1] has been applied widely. The criteria of the standard are classified by the size of the rotating machines, and each of these machines is monitored based on the vibration velocity during operation. However, in using actual machines, for example, in order not to transfer the vibration from a vehicle or a ship to the machines, or in order not to transfer the vibration from equipment in the opposite direction, equipment may be fixed non-rigidly. These machines are loosely attached on top of an exclusive stand by means of cushioning material.

In such a situation, vibrations tend to be large as compared with the case of rigidly supported equipment. Direct application of the conventional criteria is difficult, because

K. L. Cavalca and H. I. Weber (Eds.): IFToMM 2018, MMS 61, pp. 161–174, 2019.
https://doi.org/10.1007/978-3-319-99268-6_12

a large amplitude is measured even for normal machines. Therefore, the criteria of conventional evaluation methods have been expanded for some equipment, and vibration amplitude is evaluated by reference to provisional criteria.

In order to evaluate the flexibly supported equipment, this study is intended to establish an evaluation method that considers the classification of not only the size of equipment but also the stiffness or damping between the equipment base and ground. One simple disk rotor which is supported by ball bearings at both ends is prepared by reference to the previous studies [2–5]. The base of the experimental system is fixed to ground rigidly or flexibly. Numerical models of the rotor and the base of rotor were derived, and combined as a total model, and then numerical simulations were performed under flexible conditions of linear and non-linear springs. The resonance frequencies of rotor vibrations were evaluated by resonance curve derived by means of numerical simulations, in order to obtain basic data.

2 Experimental System

2.1 Rigid Support

Figure 1 shows the experimental system [6]. The experimental system consists of an aluminum base and a rotor having one disk. Disk mass is 2.2 kg. The shaft is supported by ball bearings on both ends, and is then rotated by an AC servo motor via a coupling. Vibration displacement of the shaft center is measured using an eddy current displacement meter. The rotational speed of the shaft is measured by using a notched ring mounted on the shaft for pulse measurement.

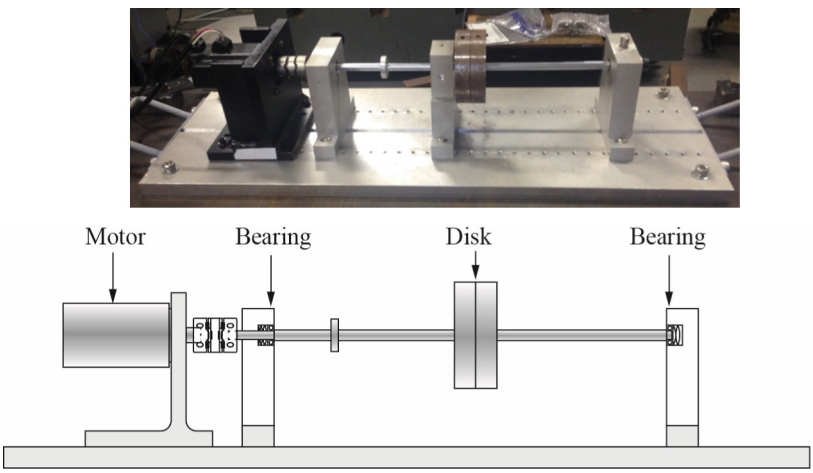

Fig. 1. Experimental system of rigid support

2.2 Support by Linear Springs

In order to evaluate the flexibly supported equipment in addition to the rigidly supported equipment, as shown in Fig. 2 [6], the base of the same experimental system is supported by four plate springs in the same simulated circumstance as for a flexible support. The plate springs are made of soft steel having a thickness of 1 mm, and have the shape shown in Fig. 3. The plate spring is used to adjust the length to support, because it can change the support stiffness. In this study, numerical calculations were performed with five springs having lengths of 10 to 50 mm in 10 mm increments.

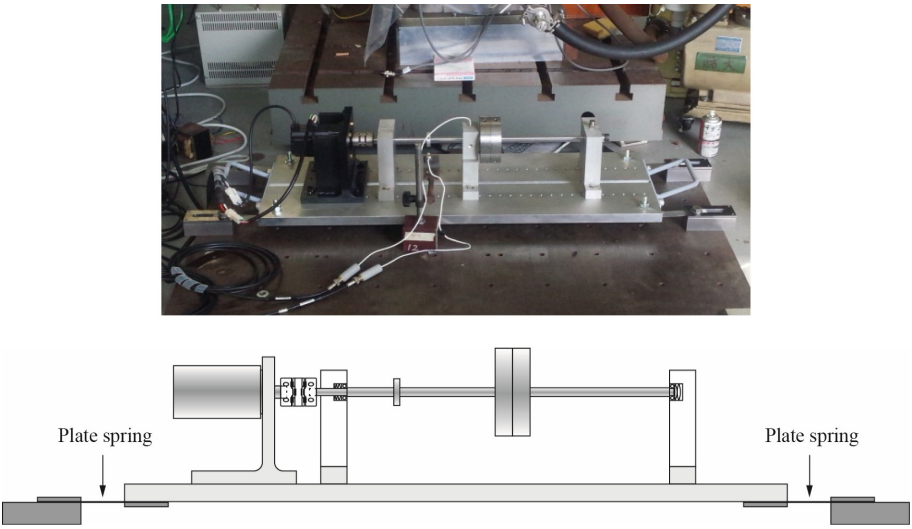

Fig. 2. Experimental system flexibly supported by plate springs (linear spring)

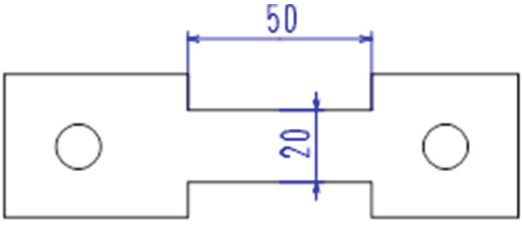

Fig. 3. Plate spring (thickness = 1[mm])

2.3 Support by Non-linear Springs

Figure 4 shows the experimental equipment supported by vibration isolating rubber members (non-linear springs). The rotating system is almost same as that shown in Fig. 2. The rubber members are made of molded silicone rubber and have non-linear

characteristics. In this study, numerical calculations were performed with added mass and added moment of inertia.

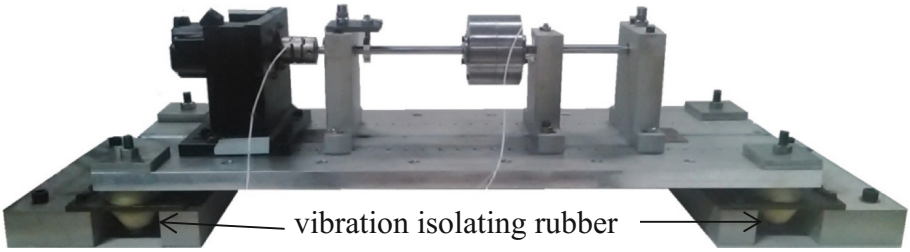

Fig. 4. Experimental system flexibly supported by vibration isolating rubber members (non-linear spring)

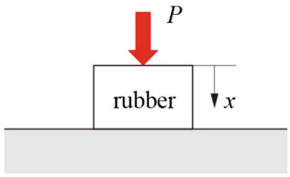

Fig. 5. Rubber spring model

2.4 Characteristics of Vibration Isolating Rubber Members

Figure 5 shows an example of rubber spring model. In the vibration isolating rubber used in this paper, the relation between load P [N] and displacement x [m] is as follows:

$$P = 10^{A+Bx} \tag{1}$$

where A and B are constants. When a large mass is set on a small rubber, the relation may be expressed in Eq. (1). Considering the spring constant of the rubber as the slope of displacement vs. load relation, the spring constant at the position where the load and the rubber reaction force are balanced is expressed as follows.

$$\frac{dP}{dx} = \ln 10 \cdot B \cdot 10^{A+Bx} = \ln 10 \cdot B \cdot P \tag{2}$$

According to Eq. 2, it can be seen that the stiffness of the rubber is proportional to the load P. Natural frequency of the rotating machine supported by the rubber is as follows:

$$\omega_n^* = \sqrt{\frac{k}{m}} = \sqrt{\frac{\ln 10 \cdot B \cdot P}{P/g}} = \sqrt{\ln 10 \cdot B \cdot g} \tag{3}$$

where m [kg] is mass of the rotating machine, g [m/s^2] is gravitational acceleration and $P = mg$. Since all the variables in Eq. 3 are constants, the natural frequency is constant regardless of the mass of the rotating machine.

3 Numerical Model and Simulations

3.1 Modeling Rotor on Rigid Support Base and Simulations

The rotor of the rotating machine is modeled by the finite element method, with the rotor divided into 25 elements. Figure 6 shows the FE model of the rotor. The equation of motion is as follows:

$$\mathbf{M}\ddot{\mathbf{X}} + \mathbf{C}\dot{\mathbf{X}} + \mathbf{K}\mathbf{X} = \mathbf{F} \tag{4}$$

M is mass matrix, C is damping matrix, and K is stiffness matrix. Gyroscopic effects are omitted in this experimental system, because the disc is located at the center of the shaft and does not tilt in the 1st mode. In this model, changes in 1st critical speed (34 Hz) due to the gyro effect are less than 0.001 Hz, while the rated speed is 60 rps. The equation of motion is transformed to a reduction model by using the mode-synthesis method [7, 8]. In this modeling method, after modeling the rotor, the rotor and the base of machine model are combined to form a total model. If the base of the machine changes, the model can be easily rebuilt. Figure 7 shows the rigid modes and inner bending modes by which the reduction model is derived from mode synthesis method. ϕ_3 mode has an asymmetric shape, because the disk is located at the center of the shaft, where mode amplitude is very small. The mode matrix is defined by these modes as follows:

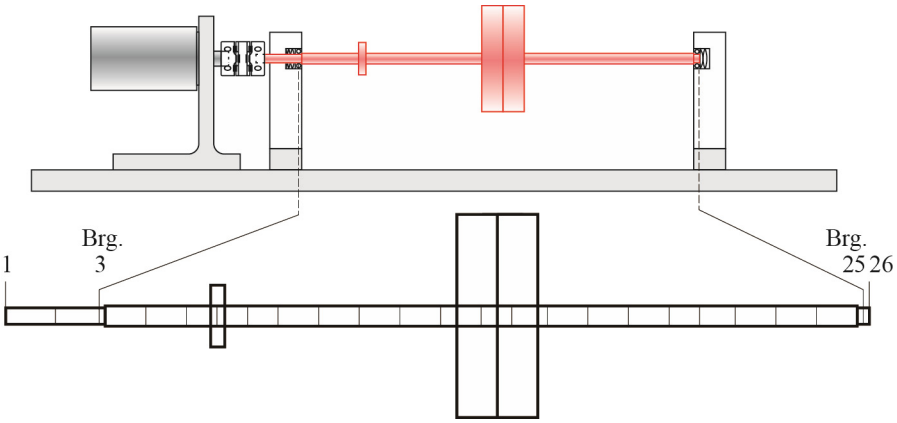

Fig. 6. FEM model

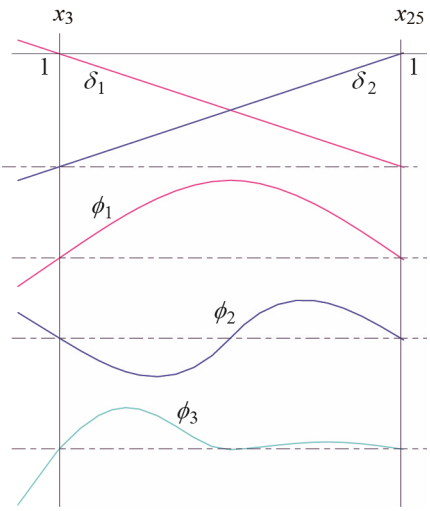

Fig. 7. Mode shape

$$\Phi = (\delta_1, \delta_2, \phi_1, \phi_2, \phi_3) \tag{5}$$

Coordinate conversion is defined as follows:

$$\mathbf{X} = \mathbf{\Phi X}_\Phi \quad \mathbf{X}_\Phi = (x_3, x_{25}, \eta_1, \eta_2, \eta_3) \tag{6}$$

x_3 and x_{25} are the coordinates of bearing positions. η_1, η_2 and η_3 are mode coordinates of bending modes. When Eqs. (5) and (6) are substituted into Eq. (4), the following mode-synthesis reduction model is obtained:

$$\mathbf{M}_\Phi \ddot{\mathbf{X}}_\Phi + \mathbf{C}_\Phi \dot{\mathbf{X}}_\Phi + \mathbf{K}_\Phi \mathbf{X}_\Phi = \mathbf{F}_\Phi \tag{7}$$

where $\mathbf{M}_\Phi = \mathbf{\Phi}^t \mathbf{M} \mathbf{\Phi}$, $\mathbf{C}_\Phi = \mathbf{\Phi}^t \mathbf{C} \mathbf{\Phi}$, $\mathbf{K}_\Phi = \mathbf{\Phi}^t \mathbf{K} \mathbf{\Phi}$, these are as follows:

$$\begin{aligned} \mathbf{M}_\Phi &= \begin{bmatrix} \delta_1^t M \delta_1 & \delta_1^t M \delta_2 & \delta_1^t M \varphi_1 & \delta_1^t M \phi_2 & \delta_1^t M \phi_3 \\ \delta_2^t M \delta_1 & \delta_2^t M \delta_2 & \delta_2^t M \varphi_1 & \delta_2^t M \phi_2 & \delta_2^t M \phi_3 \\ \phi_1^t M \delta_1 & \phi_1^t M \delta_2 & \phi_1^t M \phi_1 & \phi_1^t M \phi_2 & \phi_1^t M \phi_3 \\ \phi_2^t M \delta_1 & \phi_2^t M \delta_2 & \phi_2^t M \phi_1 & \phi_2^t M \phi_2 & \phi_2^t M \phi_3 \\ \phi_3^t M \delta_1 & \phi_3^t M \delta_2 & \phi_3^t M \phi_1 & \phi_3^t M \phi_2 & \phi_3^t M \phi_3 \end{bmatrix} \\ &= \begin{bmatrix} 0.69 & 0.61 & 0.038 & -0.0023 & 0.00020 \\ 0.61 & 0.67 & 0.038 & 0.0024 & 0.000096 \\ 0.0038 & 0.038 & 0.0023 & 0 & 0 \\ -0.0023 & 0.0024 & 0 & 0.000031 & 0 \\ 0.00020 & 0.000096 & 0 & 0 & 0.0000017 \end{bmatrix} \end{aligned} \tag{8}$$

$$\mathbf{C_\Phi} = \text{diag.}[\,c_b \quad c_b \quad 0.03 \quad 0.15 \quad 0.15\,] \tag{9}$$

$$\mathbf{K_\Phi} = \text{diag.}[\,k_b \quad k_b \quad 88 \quad 515 \quad 481\,] \tag{10}$$

where c_b is bearing damping coefficient, and k_b is bearing stiffness. If $k_b = 8.0 \times 10^6$ N/m, the natural frequencies from the first mode to the third mode are 34.6 Hz, 250 Hz, and 846 Hz, respectively. In this model, changes in 1st critical speed due to gyro effect are less than 0.001 Hz, since the disc is located at the center of the shaft and does not tilt in the 1st mode. Therefore we ignore the gyro effect in this paper. In the case of $c_b = 60.4$ Ns/m, the response curve of unbalance is obtained as Fig. 8.

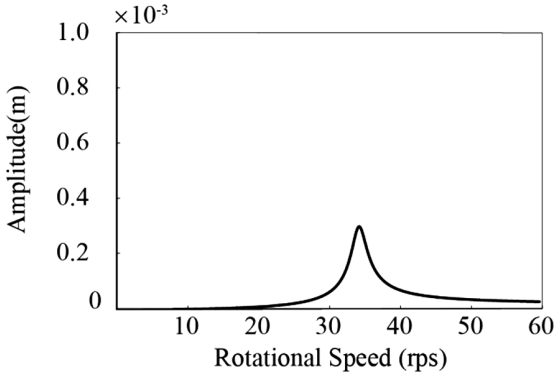

Fig. 8. Resonance curve of rigid support in numerical simulation

3.2 Modeling Rotor on Flexibly Support Base by Linear Springs

In order to model the rotor and flexible support base together, it is necessary to consider the motion of the machine base which supports rotating parts. In Fig. 9, translating and tilting motions of the center of gravity of the base are expressed as follows:

$$\begin{bmatrix} m & 0 \\ 0 & I_G \end{bmatrix} \begin{bmatrix} \ddot{x}_G \\ \ddot{\theta}_G \end{bmatrix} + \begin{bmatrix} 2c_g & -(a-b)c_g \\ -(a-b)c_g & (a^2+b^2)c_g \end{bmatrix} \begin{bmatrix} \dot{x}_G \\ \dot{\theta}_G \end{bmatrix} + \begin{bmatrix} 2k_g & -(a-b)k_g \\ -(a-b)k_g & (a^2+b^2)k_g \end{bmatrix} \begin{bmatrix} x_G \\ \theta_G \end{bmatrix} = \begin{bmatrix} F_G \\ M_G \end{bmatrix} \tag{11}$$

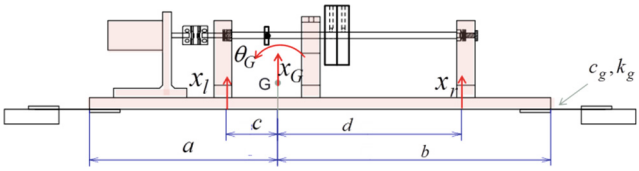

Fig. 9. Experimental equipment Model (flexible support by linear springs)

The translating and tilting motions are transformed to the motions of the bearing positions, and Eq. (11) is expressed by using x_l and x_r as bearing coordinates as follows:

$$\begin{aligned}&\left(\frac{1}{c+d}\right)^2\begin{bmatrix} d & c \\ -1 & 1 \end{bmatrix}^T\begin{bmatrix} m & 0 \\ 0 & I_G \end{bmatrix}\begin{bmatrix} d & c \\ -1 & 1 \end{bmatrix}\begin{bmatrix} \ddot{x}_l \\ \ddot{x}_r \end{bmatrix} \\ &+\left(\frac{1}{c+d}\right)^2\begin{bmatrix} d & c \\ -1 & 1 \end{bmatrix}^t\begin{bmatrix} 2c_g & -(a-b)c_g \\ -(a-b)c_g & (a^2+b^2)c_g \end{bmatrix}\begin{bmatrix} d & c \\ -1 & 1 \end{bmatrix}\begin{bmatrix} \dot{x}_l \\ \dot{x}_r \end{bmatrix} \\ &+\left(\frac{1}{c+d}\right)^2\begin{bmatrix} d & c \\ -1 & 1 \end{bmatrix}^t\begin{bmatrix} 2k_g & -(a-b)k_g \\ -(a-b)k_g & (a^2+b^2)k_g \end{bmatrix}\begin{bmatrix} d & c \\ -1 & 1 \end{bmatrix}\begin{bmatrix} x_l \\ x_r \end{bmatrix} = \begin{bmatrix} F_l \\ F_r \end{bmatrix}\end{aligned} \tag{12}$$

where m and I_G are the mass and the moment of inertia about the center of gravity of the experimental system not including the rotor, and c_g and k_g are damping coefficient and stiffness between base and ground, respectively.

Mass matrix, damping matrix, and stiffness matrix in Eq. (12) are defined as $\mathbf{M}_b$, $\mathbf{C}_b$, and $\mathbf{K}_b$, respectively, and equation of motion is expressed as follows:

$$\mathbf{M}_b\begin{bmatrix} \ddot{x}_l \\ \ddot{x}_r \end{bmatrix} + \mathbf{C}_b\begin{bmatrix} \dot{x}_i \\ \dot{x}_r \end{bmatrix} + \mathbf{K}_b\begin{bmatrix} x_i \\ x_r \end{bmatrix} = \begin{bmatrix} F_l \\ F_r \end{bmatrix} \tag{13}$$

Equation (7) serving as the reduction model of the rotor and Eq. (13) serving as the base model are combined by using bearing damping c_b and stiffness k_b. Mass matrix, damping matrix, and stiffness matrix of the total system are defined as $\mathbf{M}_{all}$, $\mathbf{C}_{all}$, and $\mathbf{K}_{all}$, respectively, and equation of motion of the total system is expressed as follows:

$$\mathbf{M}_{all}\begin{bmatrix} \ddot{\mathbf{X}}_\Phi \\ \ddot{x}_l \\ \ddot{x}_r \end{bmatrix} + \mathbf{C}_{all}\begin{bmatrix} \dot{\mathbf{X}}_\Phi \\ \dot{x}_l \\ \dot{x}_r \end{bmatrix} + \mathbf{K}_{all}\begin{bmatrix} \ddot{\mathbf{X}}_\Phi \\ \ddot{x}_l \\ \ddot{x}_r \end{bmatrix} = \begin{bmatrix} \mathbf{F}_\Phi \\ F_l \\ F_r \end{bmatrix} \tag{14}$$

where $\mathbf{M}_{all}$, $\mathbf{C}_{all}$, and $\mathbf{K}_{all}$ are expressed as follows:

$$\mathbf{M}_{all} = \begin{bmatrix} \mathbf{M}_\Phi & \mathbf{0} \\ \mathbf{0} & \mathbf{M}_b \end{bmatrix} \tag{15}$$

$$\mathbf{C}_{all} = \begin{bmatrix} c_b & 0 & 0 & 0 & 0 & -c_b & 0 \\ 0 & c_b & 0 & 0 & 0 & 0 & -c_b \\ 0 & 0 & 0.03 & 0 & 0 & 0 & 0 \\ 0 & 0 & 0 & 0.15 & 0 & 0 & 0 \\ 0 & 0 & 0 & 0 & 0.15 & 0 & 0 \\ -c_b & 0 & 0 & 0 & 0 & c_b + 2.8_{c_g} & 1.6_{c_g} \\ 0 & -c_b & 0 & 0 & 0 & -1.6_{c_g} & c_s + 2.4_{c_g} \end{bmatrix} \tag{16}$$

$$\mathbf{K}_{all} = \begin{bmatrix} k_b & 0 & 0 & 0 & 0 & -k_b & 0 \\ 0 & k_b & 0 & 0 & 0 & 0 & -k_b \\ 0 & 0 & 88 & 0 & 0 & 0 & 0 \\ 0 & 0 & 0 & 515 & 0 & 0 & 0 \\ 0 & 0 & 0 & 0 & 481 & 0 & 0 \\ -k_b & 0 & 0 & 0 & 0 & k_b + 2.8k_b & 1.6k_b \\ 0 & -k_b & 0 & 0 & 0 & -1.6k_b & c_s + 2.4k_b \end{bmatrix} \tag{17}$$

Eight c_b are inserted manually in damping matrix (Eq. (16)) to connect x_l of the base to x_3 of the shaft and to connect x_r and x_{25}. In the same manner, eight k_b are inserted in stiffness matrix (Eq. (17)) to connect these coordinates. c_g and k_g are damping coefficient and stiffness of the plate springs. c_g is 5.0 Ns/m, as measured by a hammering test (Table 1).

Table 1. Simulation conditions (linear spring)

	Length L [mm]	Spring constant k_g [N/m]
case a1	10	7.15×10^5
case a2	20	3.47×10^5
case a3	30	2.07×10^5
case a4	40	1.50×10^5
case a5	50	1.23×10^5

In simulations, response curves of unbalance are obtained when the length of the plate spring changes. Figure 10 shows response curve in changing the stiffness corresponding to the plate springs (L = 10–50 mm). The stiffness for L = 10 mm is the largest, and that for L = 50 mm is the lowest. In the case of the rigidly supported base, a large amplitude value exists at the natural frequency of the rotor, but in the case of flexible support, three large amplitude values exist, at the natural frequencies of the translating and tilting of the flexible supported base in addition to that of the rotor. When the base is supported by a plate spring as L = 10 mm, two peaks exist, because the highest natural frequency of the base is beyond the range of rotational speed. These figure machine conditions are good, but large amplitude values are measured at certain rotational speeds because of the base vibration. Therefore, in the case of using linear springs the spring constant must be selected so that the frequency of the base does not coincide with the rated rotation speed (Table 2).

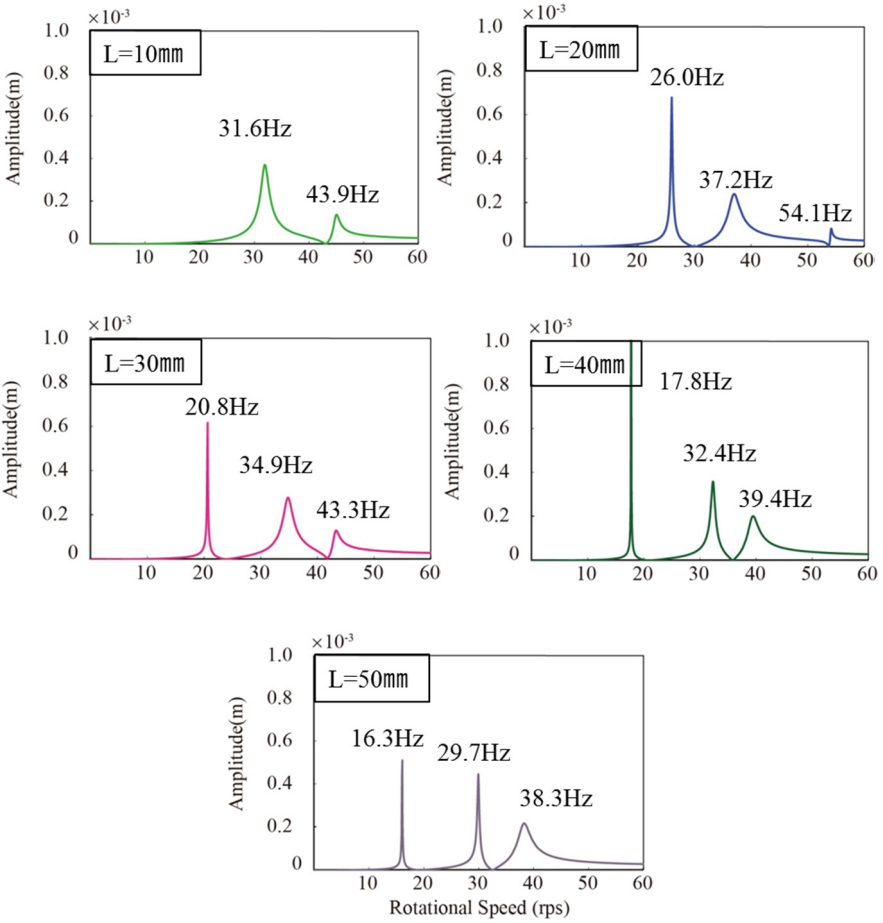

Fig. 10. Resonance curve of flexible support in numerical simulations (linear springs)

Table 2. Resonance frequencies (linear spring)

	Translating mode of base [Hz]	Tilting mode of base [Hz]	Bending mode of rotor [Hz]
case a1	43.9	upper 60 Hz	31.6
case a2	37.2	54.1	26.0
case a3	20.8	43.3	34.9
case a4	17.8	32.4	39.4
case a5	16.3	29.7	38.3

3.3 Modeling Rotor on Flexibly Support Base by Non-linear Springs and Simulations

Figure 11 shows the experimental model supported by vibration isolating rubber members. In the case of the numerical model using non-linear springs, $k_g = 0$, $c_g = 0$ in Eqs. (16), (17) and F_l and F_r in Eq. (14) consists of reaction force of rubber and gravity force. These forces are expressed as follows:

$$\begin{bmatrix} F_l \\ F_r \end{bmatrix} = \begin{bmatrix} 1 & 1 \\ -c & d \end{bmatrix}^{-1} \begin{bmatrix} 1 & 1 \\ -a & b \end{bmatrix} \begin{bmatrix} F_{ll} \\ F_{rr} \end{bmatrix} - \begin{bmatrix} \frac{d}{c+d} mg \\ \frac{c}{c+d} mg \end{bmatrix} \tag{18}$$

$$\begin{aligned} F_{ll} &= 2 \cdot 10^{A - Bx_{ll}} \\ F_{rr} &= 2 \cdot 10^{A - Bx_{rr}} \end{aligned} \tag{19}$$

where F_{ll} and F_{rr} are reaction force of the rubber members (left and right).

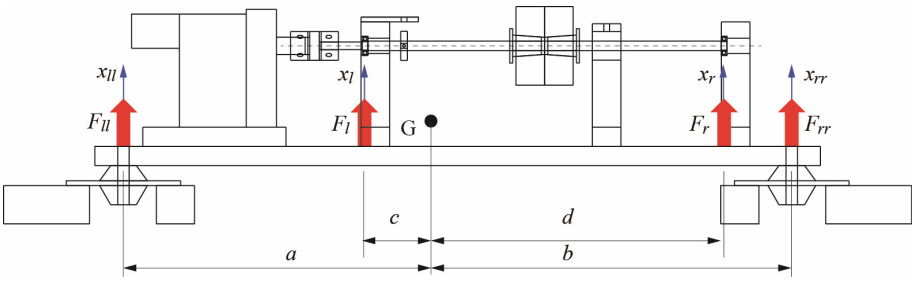

Fig. 11. Experimental equipment Model (flexible support by non-linear springs)

Numerical calculations using the rubber springs can be performed by linearizing the spring constant at the balance point of gravity, but in order to be able to calculate various nonlinear springs in the future, calculations are performed without linearizing the spring constant.

Table 3. Simulation conditions (non-linear spring)

		Mass [kg]	Moment of inertia [kg m^2]
case b1		23.2	0.90
case b2	mass addition	29.8	0.90
case b3	moment of inertia addition.	29.8	1.59

The following three types of numerical calculations were performed (Table 3).

– case b1: The mass of the experimental system is 23.2 kg and moment of inertia is 0.90 kg m^2.

– case b2: Mass (6.6 kg) is added at the center of gravity, making total mass 29.8 kg. The moment of inertia is the same as in case b1.
– case b3: Total mass is the same as in case b2. Added mass moves from the center of gravity, making the moment of inertia 1.59 kg m^2

Figures 12, 13 and 14 show the results of numerical calculations for cases b1, b2 and b3, respectively. Table 4 shows the resonance frequencies of resonance curve. In the case b1, resonance frequency of the base translating mode is 16.6 Hz, that of the base tilting mode is 30.0 Hz and that of the rotor bending mode is 45.8 Hz. In the case of b2, the resonance frequencies of base translating mode and rotor bending mode are the same as in case b1. The base tilting mode is 33.8 Hz. This result shows that the frequency does not change even if the mass increases. On the other hand, the tilting mode frequency changes. In the case of b3, the resonance frequency of the base translating mode is the same as that for cases b1 and b2. The rotor bending mode is almost the same as in cases b1 and b2. The tilting mode is 24.7 Hz. The result of case b3 shows that when the moment of inertia changes, the tilting mode frequency changes but the translating frequency does not change.

Therefore, when the rotating machine is supported by rubber having nonlinear characteristics, the resonance frequency of the translating mode does not change with the mass and the moment of inertia, but the natural frequency of the tilt mode changes. When the mass or the moment of inertia of a machine changes, it is necessary to pay attention to changes in resonance frequencies.

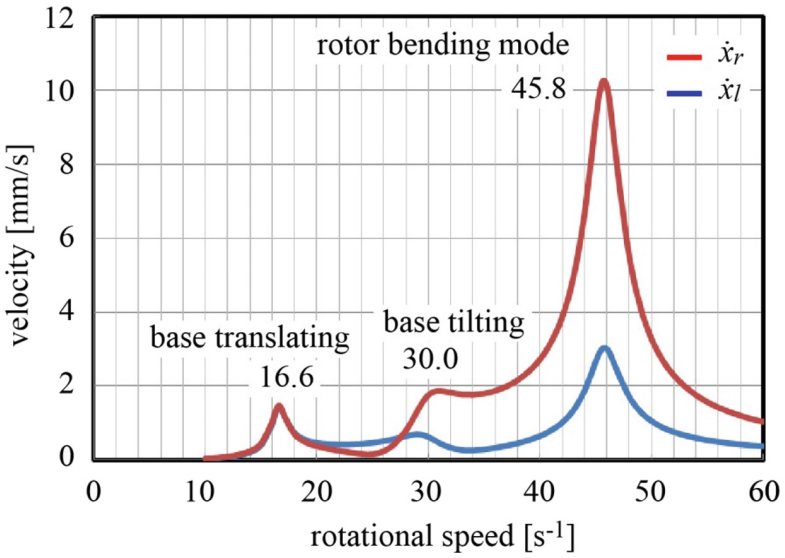

Fig. 12. Resonance curve of case b1 (non-linear spring support)

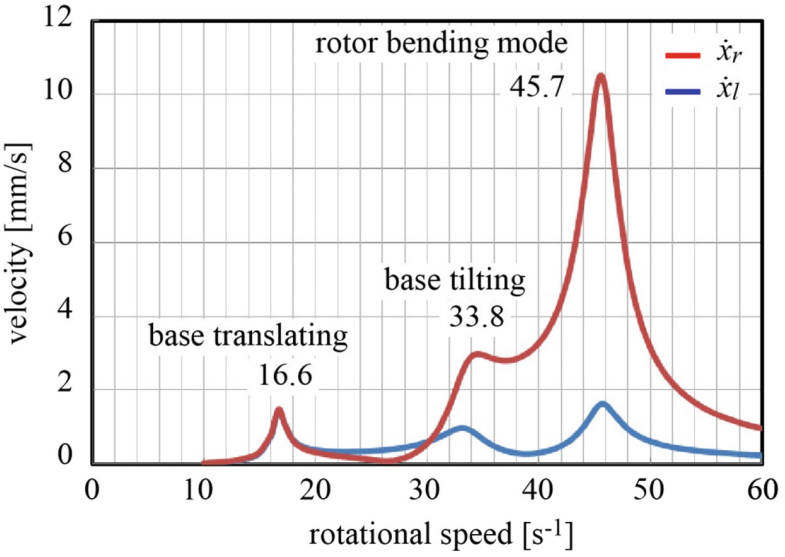

Fig. 13. Resonance curve of case b2 (non-linear spring support)

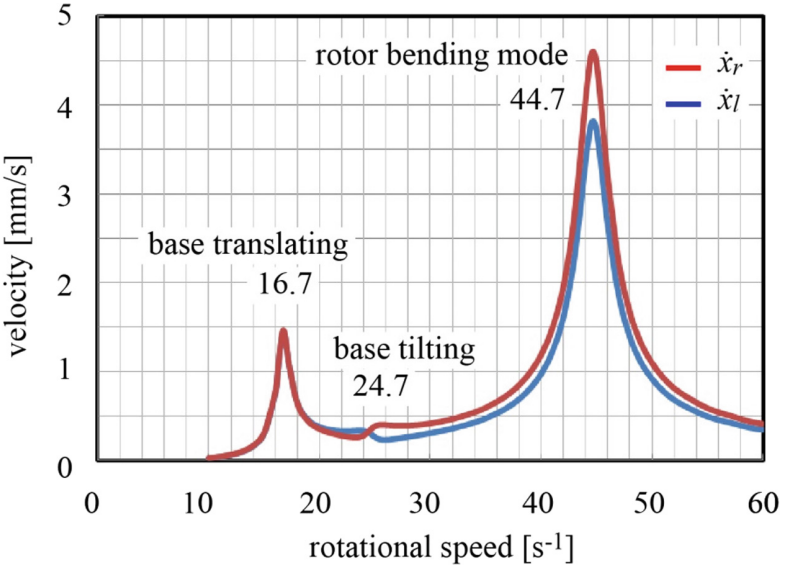

Fig. 14. Resonance curve of case b3 (non-linear spring support)

Table 4. Resonance frequencies (non-linear spring)

	Translating mode of base [Hz]	Tilting mode of base [Hz]	Bending mode of rotor [Hz]
case b1	16.6	30.0	45.8
case b2	16.7	33.8	45.7
case b3	16.7	45.7	44.7

4 Conclusions

In this paper, numerical calculations were performed with respect to rigid and flexible support experimental systems. By using the mode-synthesis method, at rotor and a base were respectively modeled and a total model was derived by combining the two models. In the case of using linear springs, the spring constant must be selected so that the frequency of the base does not coincide with the rated rotation speed. In the case of using nonlinear springs, the frequency of the translational mode does not change, but since the tilting mode changes, it must be set so that it does not coincide with the rotational speed.

References

1. ISO10816-1, Mechanical vibration - Evaluation of machine vibration by measurements on non-rotating parts
2. Edwards, S., Lees, A.W., Friswell, M.I.: Experimental Identification of excitation and support parameters of a flexible rotor-bearings-foundation system from a single run-down. J. Sound Vib. **232**(5), 963–992 (2000)
3. Han, Q., Dong, X., Wen, B.: Resonance capture of rotor system mounted on an elastically supported base. In: The 8th IFToMM International Conference on Rotor Dynamics 2010, pp. 904–910 (2010)
4. Yu, M., Feng, N., Hahn, E.: Identification of foundations in rotating machinery using modal parameters. In: IMechE Tenth International Conference on Vibrations in Rotating Machinery (VIRM10), C1326/002 (2012)
5. Zapomel, J., Ferfecki, P.: Investing of the vibration reduction of a flexibly supported Jeffcott rotor damped by semiactive elements working on th epriciple of squeezing thin layers of normal and magnetorheological oils. In: IMechE Tenth International Conference on Vibrations in Rotating Machinery (VIRM10), C1326/017 (2012)
6. Fujiwara, H., Nakaura, H., Watanabe, K.: The vibration behavior of flexibly fixed rotating machines. In: IFToMM 14th World Congress in Mechanism and Machine Science, OS14-023 (2015)
7. Ito, M., Matsushita, O., Okubo, H., Fujiwara, H.: Unbalance vibration control for high order bending critical speeds of flexible rotor supported by active magnetic bearing. In: Proceedings of the 8th International Symposium on Transport Phenomena and Dynamics of Rotating Machinery, vol. 1, pp. 923–929 (2000)
8. Ito, M., Fujiwara, H., Matsushita, O., Takahashi, N.: Control of over-hung rotor supported by active magnetic bearings. In: Proceedings of the 2nd International Symposium on Stability Control of Rotating Machinery, pp 252–260 (2003)